ROBUST ALTITUDE ESTIMATION FOR OVER-THE-HORIZON RADAR USING A STATE-SPACE MODEL FOR MULTIPATH FADING

Richard H. Anderson, Shawn Kraut and Jeffrey L. Krolik

Department of Electrical and Computer Engineering
Duke University, Durham, NC 27708-0291

ABSTRACT

In previous work, a matched-field estimate of aircraft altitude from multiple over-the-horizon radar dwells was presented. This approach exploits the altitude dependence of direct and surface reflected returns off the aircraft and the relative phase changes of these micro-multipath arrivals across radar dwells. Since this previous approach assumed high dwell-to-dwell predictability, it is sensitive to mismatch between modeled versus observed micro-multipath phase and amplitude changes from dwell-to-dwell. In this paper, a generalized matched-field altitude estimate is presented based on a state-space model that accounts for random ionospheric and target-motion effects which degrade the dwell-to-dwell predictability of target returns. The new formulation results in an efficient, robust recursive maximum likelihood altitude estimate. Simulation and real data results suggest that the proposed technique can achieve an accuracy within 5,000 ft. using 10-20 dwells, even with relatively high levels of uncertainty in modeling of dwell-to-dwell changes in the target return.

1. INTRODUCTION

Over-the-horizon (OTH) radar performs detection and tracking of long-range targets which are beyond the range of conventional line-of-sight radars. Currently, OTH radars are capable of localizing aircraft targets in ground range and azimuth but reliable altitude estimation has not been implemented to date [1, 2]. In previous work, a matched-field approach was developed for maximum likelihood estimation of aircraft altitude from multiple radar dwells based on the micro-multipath geometry of the aircraft and the ground [3, 4]. Matched field processing is a well known method for underwater source localization [5], but is fairly recent in radar applications [6]. Since the previous matched-field approach relied heavily on the dwell-to-dwell variations in the target response, it could be sensitive to mismatch between the observed complex range-Doppler data and the model of the dwell-to-dwell predictability of the micro-multipath target reflection coefficients due to target motion. In this paper, the multiple dwell maximum likelihood (ML) altitude estimate is extended to be more robust to mismatch in the modeled dwell-to-dwell changes versus the observed dwell-to-dwell changes in the target response.

The robust multiple dwell matched-field altitude estimation approach described here accounts for uncertainty in the dwell-to-dwell phase changes of the complex target amplitudes for each micro-multipath by the inclusion of a random complex target amplitude component that is uncorrelated from dwell to dwell. The resulting time-evolving log-likelihood includes dependence of the data on all the previous dwells rather than just the previous dwell. The scaling of the random dwell-to-dwell target complex amplitude changes is adapted by matching the magnitude of the prediction errors to the prediction error covariance. The micro-multipath model of the complex range-Doppler data with uncertainty in the dwell-to-dwell complex target reflection coefficients is presented in Section 2. A recursive method for computing the log-likelihood over multiple dwells is derived in Section 3. In Section 4, Monte Carlo simulations and results with real data suggest that robust altitude estimation to within 5,000 ft. accuracy can be achieved after a few dwells, even in the presence of uncertainty in the dwell-to-dwell predictability of the micro-multipath target reflection amplitudes.

This work was sponsored by ONR under grant N00014-99-1-0532.

2. MICRO-MULTIPATH MODEL WITH UNCERTAINTY

In this section, the model of the time-evolving target return in complex range-Doppler space is derived for each micro-multipath to altitude z. Since OTH radars successfully associate peaks with slant tracks and routinely estimate target ground range, velocity and azimuth, both the slant-track-to-peak association and the target location parameters are assumed to be known *a priori* [7]. Further it is assumed that "baseline" ionospheric ray path predictions of elevation angle and slant range to the target ground range at $z = 0$ are known *a priori*. For a bistatic OTH radar, the target return contains contributions from the $L = 4$ micro-multipath combinations shown in Figure 1.

The signal model is developed for an $N \times M$ block of the complex range-Doppler surface centered around the slant range and Doppler frequency for the target return of interest. Converting the $N \times M$ block of data to a $NM \times 1$ vector, the component of the target return along the lth micro-multipath ray is given by the product $\mathbf{h}_{l,k}(z)x_{l,k}$ where $\mathbf{h}_{l,k}(z)$ is the complex transfer function of the radar in range-Doppler space and $x_{l,k}$ is a random complex target reflection coefficient due to the unknown reflections off the aircraft and ground. In previous work [3], $x_{l,k}$ was assumed to vary slowly from dwell $k-1$ to dwell k due to the deterministic phase change $\exp[j\omega_{l,k}(z)\Delta\tau_k]$ where $\omega_{l,k}(z)$ is the average Doppler frequency along the lth micro-multipath ray and $\Delta\tau_k$ is the time interval between dwells $k-1$ and k. In this paper, we remove this simplification and model the dwell-to-dwell change $x_{l,k}$ as a combination of the predictable Doppler phase change above plus a random complex amplitude change, $v_{l,k}$. The random component accounts for modeling errors in the target motion and micro-multipath geometry, i.e. errors in the target Doppler frequencies due to target altitude and/or aspect changes, errors in ray elevation angles, etc. [4]. Letting $\mathbf{x}_k$ denote the 4×1 vector of micro-multipath target reflection coefficients, we can write its

dwell-to-dwell evolution as

$$\mathbf{x}_k = \mathbf{A}_k(z)\ \mathbf{x}_{k-1} + b_k \mathbf{v}_k, \tag{1}$$

where $\mathbf{A}_k(z)$ is diagonal with $[\mathbf{A}_k(z)]_{l,l} = e^{j\omega_{l,k}(z)\Delta\tau_k}$ and where b_k is an adjustable scaling of $\mathbf{v}_k$. The random component, $\mathbf{v}_k$, is which is assumed to be zero-mean Gaussian distributed with covariance $\mathbf{K}_{vv}$ and to be uncorrelated from dwell to dwell. In terms of $\mathbf{x}_k$, the observed $NM \times 1$ target return data, $\mathbf{y}_k$, at dwell k can be written as

$$\mathbf{y}_k = e^{j\theta_k}\ \mathbf{H}_k(z)\ \mathbf{x}_k + \mathbf{n}_k, \tag{2}$$

where θ_k is the unknown starting phase of the dwell, the lth column of $\mathbf{H}_k(z)$ is $\mathbf{h}_{l,k}(z)$ and $\mathbf{n}_k$ represents additive noise which is assumed to be zero mean Gaussian distributed with covariance $\mathbf{R}_k$ and to be uncorrelated from dwell to dwell.

3. RECURSIVE ALTITUDE ESTIMATION

Let the set of data observations for dwells 1 to K be denoted by $\mathbf{y}_{1:K}$. The maximum likelihood estimate of altitude is formed by maximizing the joint distribution of $\mathbf{y}_{1:K}$ conditioned on altitude and the unknown phases, $\theta_{1:K} = [\theta_1, \ldots, \theta_K]$, i.e. maximizing

$$\log p(\mathbf{y}_{1:K}|z, \theta_{1:K}) = \sum_{k=1}^{K} \log p(\mathbf{y}_k|\mathbf{y}_{1:k-1}, z, \theta_k) \tag{3}$$

with respect to z and $\theta_{1:K}$, where $p(\mathbf{y}_k|\mathbf{y}_{1:k-1}, z, \theta_k)$ is the distribution of $\mathbf{y}_k$ conditioned on the data from all the previous dwells. In the previous altitude estimation approach, this distribution was approximated by $p(\mathbf{y}_k|\mathbf{y}_{k-1}, z, \theta_k)$ which is conditioned on just the data from previous dwell [3]. Note that since $\mathbf{v}_k$ and $\mathbf{n}_k$ are both Gaussian, then the conditional distribution of $\mathbf{y}_k$ is also Gaussian and the conditional log-likelihood can be written as

$$\begin{aligned}\log p(\mathbf{y}_k|\mathbf{y}_{1:k-1}, z, \theta_k) = &-\log\left(\pi^{NM}|\mathbf{Q}_k(z)|\right) \\ &- \left(\mathbf{y}_k - \widehat{\mathbf{y}}_{k|k-1}(z,\theta_k)\right)^\dagger \mathbf{Q}_k^{-1}(z)\left(\mathbf{y}_k - \widehat{\mathbf{y}}_{k|k-1}(z,\theta_k)\right),\end{aligned} \tag{4}$$

where the mean $\widehat{\mathbf{y}}_{k|k-1}(z,\theta_k)$ and covariance $\mathbf{Q}_k(z)$ are conditioned on all the previous data $\mathbf{y}_{1:k-1}$. Under the model in (1) and (2), the conditional mean and covariance of the data can be computed recursively with a modified form of the Kalman filter for each hypothesized altitude. The state vector corresponds to $\mathbf{x}_k$ and this recursive computation includes a step for adapting the scaling parameter, b_k, i.e. the process noise variance. It is important to note that the objective of this approach is not estimation of the state vector $\mathbf{x}_k$, which is essentially a nuisance parameter, but rather is to form the measurement prediction, $\widehat{\mathbf{y}}_{k|k-1}$, and covariance, $\mathbf{Q}_k$, for computing the log-likelihood in (4) and the sum in (3) at each hypothesized altitude.

Suppressing the dependence on hypothesized altitude z, the recursion can be started where $\widehat{\mathbf{y}}_{k|k-1}$, $\mathbf{Q}_k$, $\widehat{\theta}_k$ and b_k^2 have been previously computed as well as the mean, $\widehat{\mathbf{x}}_{k|k-1}$, and covariance, $\mathbf{S}_{k|k-1}$, of $\mathbf{x}_k$ which are both conditioned on the previous data $\mathbf{y}_{1:k-1}$. The updated mean and covariance of $\mathbf{x}_k$ conditioned on all the data, $\mathbf{y}_{1:k}$, are given by

$$\widehat{\mathbf{x}}_{k|k} = \widehat{\mathbf{x}}_{k|k-1} + \mathbf{S}_{k|k-1}(e^{j\widehat{\theta}_k}\mathbf{H}_k)^\dagger \mathbf{Q}_k^{-1}\boldsymbol{\nu}_k \tag{5}$$

$$\mathbf{S}_{k|k} = \mathbf{S}_{k|k-1} - \mathbf{S}_{k|k-1}\mathbf{H}_k^\dagger \mathbf{Q}_k^{-1}\mathbf{H}_k\mathbf{S}_{k|k-1} \tag{6}$$

where $\boldsymbol{\nu}_k = (\mathbf{y}_k - \widehat{\mathbf{y}}_{k|k-1})$ is the prediction error used to correct the estimate of $\mathbf{x}_k$ with data $\mathbf{y}_k$. The predicted mean and covariance of $\mathbf{x}_{k+1}$ conditioned on $\mathbf{y}_{1:k}$ are given by

$$\begin{aligned}\widehat{\mathbf{x}}_{k+1|k} &= \mathbf{A}_k\widehat{\mathbf{x}}_{k|k} \\ \mathbf{S}_{k+1|k} &= \mathbf{A}_k\mathbf{S}_{k|k}\mathbf{A}_k^\dagger + b_k^2\mathbf{K}_{vv}\end{aligned}$$

Since the measurement prediction error covariance,

$$\mathbf{Q}_{k+1} = \mathbf{H}_k\mathbf{S}_{k+1|k}\mathbf{H}_k^\dagger + \mathbf{R}_{k+1}, \tag{7}$$

is independent of θ_{k+1}, it can be used to form the maximum likelihood estimate of the starting phase

$$e^{j\widehat{\theta}_{k+1}} = \frac{\widehat{\mathbf{x}}_{k+1|k}^\dagger \mathbf{H}_{k+1}^\dagger \mathbf{Q}_{k+1}^{-1}\mathbf{y}_{k+1}}{\left|\widehat{\mathbf{x}}_{k+1|k}^\dagger \mathbf{H}_{k+1}^\dagger \mathbf{Q}_{k+1}^{-1}\mathbf{y}_{k+1}\right|} \tag{8}$$

where the dependence of θ_{k+1} on data other than $\mathbf{y}_{k+1}$ is neglected. With this estimate of θ_{k+1}, the measurement prediction at dwell $k+1$ is given by $\widehat{\mathbf{y}}_{k+1|k} = e^{j\widehat{\theta}_{k+1}}\mathbf{H}_k\widehat{\mathbf{x}}_{k+1|k}$.

The final step in the recursion is to adaptively adjust the scaling term b_{k+1}^2 based on $\mathbf{y}_{k+1}$. The approach to this scaling adjustment is based on the observation that $E[||\boldsymbol{\nu}_{k+1}||^2] = \text{tr}(\mathbf{Q}_{k+1})$ so large differences between $||\boldsymbol{\nu}_{k+1}||^2$ and $\text{tr}(\mathbf{Q}_{k+1})$ indicate a significant modeling discrepancy [8]. Therefore b_{k+1}^2 is chosen such that $||\boldsymbol{\nu}_{k+1}||^2 = \text{tr}(\mathbf{Q}_{k+1})$. By substituting $||\boldsymbol{\nu}_{k+1}||^2$ for its expected value and rewriting

$$\mathbf{Q}_{k+1} = \mathbf{H}_k\mathbf{A}_k\mathbf{S}_{k|k}\mathbf{A}_k^\dagger\mathbf{H}_k^\dagger + b_{k+1}^2\mathbf{H}_k\mathbf{K}_{vv}\mathbf{H}_k^\dagger + \mathbf{R}_{k+1},$$

the estimated process noise variance scaling is given by

$$\widehat{b}_{k+1}^2 = \frac{||\boldsymbol{\nu}_{k+1}||^2 - \text{tr}\left(\mathbf{H}_k\mathbf{A}_k\mathbf{S}_{k|k}\mathbf{A}_k^\dagger\mathbf{H}_k^\dagger + \mathbf{R}_{k+1}\right)}{\text{tr}(\mathbf{H}_k\mathbf{K}_{vv}\mathbf{H}_k^\dagger)} \tag{9}$$

To ensure that this scaling parameter is both non-negative and commensurate with the scale of the data, the adapted scaling is given by $b_{k+1}^2 = \max[\,\widehat{b}_{k+1}^2, a\,||\boldsymbol{\nu}_{k+1}||^2/\text{tr}(\mathbf{H}_k\mathbf{K}_{vv}\mathbf{H}_k^\dagger)]$ where $0 < a \leq 1$ and a is a specified parameter to control the minimum setting of b_{k+1}^2. A setting of $a = 1/8$ is used for the simulation and real data results in Section 4.

Note that while the dwell-to-dwell variations in the target response amplitude are indirectly handled by adapting b_k^2, this adaptation has an inherent 1 dwell lag behind the measurement prediction. Further, this approach does not account for modeling mismatch in the columns of $\mathbf{H}_k(z)$ in (2) due to effects such as radar calibration errors, or delay spread from polarization dependent ionospheric propagation paths, i.e. extraordinary and ordinary rays.

4. PERFORMANCE RESULTS

In this section, the performance of the recursive maximum likelihood altitude estimate is evaluated by simulation of a typical OTH radar aircraft track. The distributions of the estimates over 200 Monte Carlo simulations are computed as a function of the true altitude and the number of dwells. The simulated radar signal consisted of a series of linear FM chirps with a bandwidth of 8.3 kHz, a nominal coherent integration time of 2.5 seconds, a nominal waveform repetition frequency of 52 Hz and a radar operating frequency at 18.95 MHz. The target slant range was between 1800 and 2000

km and its radial velocity was roughly 330 knots. The revisit interval between dwells was 30 to 40 seconds. The baseline ionospheric ray path was modeled with numerical ray tracing through a range-dependent ionosphere with plasma frequency parameters estimated from *in-situ* ionograms.

Figure 2 shows an example of the log-likelihood in (3) over 33 dwells for a true target altitude of 29,500 ft and a signal-to-noise ratio (SNR) of 20 dB. The scaling parameter, b_k^2, was set to one in the generation of the simulated data. This corresponds to roughly equal random and non-random components in (1) and thus significant uncertainty in the dwell-to-dwell predictability of $\mathbf{x}_k$. The estimate at each dwell is indicated by the circle symbols and the true altitude by the dashed line. Note that while altitude ambiguities in the log-likelihood persist for more than 20 dwells, the estimate converges to the true altitude within 6 dwells. The altitude ambiguities correspond to aliasing in altitude due to undersampling in revisit interval for this fast commercial aircraft.

Figure 3 shows the histogram of the altitude estimates in log probability for 200 Monte Carlo simulations at 20 dB SNR with a true aircraft altitude of 29,500 ft. The estimates are very widely distributed for the first few dwells where the data is limited. Figure 3 shows that the estimates are consistently close to the true altitude from dwell 5 on. Figures 4 and 5 show similar histograms for simulations with true altitudes of 19,700 and 9,800, respectively. While the distributions of the estimates certainly becomes wider for lower flying aircraft, the histograms suggest that accurate altitude estimation can be achieved within 10 to 20 dwells at lower altitudes.

Figure 6 shows the log-likelihood surface from processing the real OTH radar data of a commercial aircraft. The average SNR of the target peaks was roughly 20 dB. The estimate at each dwell is indicated by a circle and the true altitude is shown by the dashed line. In 7 dwells, the altitude estimate converges to within 300 ft. of the true altitude of 29,000 ft. The estimates remain very close to the true altitude until the last few dwells when no detected peaks were associated with this track. In contrast, the altitude estimates from previous work for this track were consistently high by over 6,000 ft. and further predicted very small log-likelihoods at the true altitude. For this real data example, the approach presented here provides a clear accuracy improvement in the altitude estimate over the previous technique.

5. CONCLUSIONS

In this paper, a maximum likelihood estimate of aircraft altitude for OTH radar was derived for a micro-multipath model with uncertainty in the dwell-to-dwell predictability of the complex target reflection coefficients. Simulation results indicate that accurate altitude estimation can be achieved with a limited number of radar dwells at a moderate SNR and a quite high level of uncertainty in the dwell-to-dwell predictability of the micro-multipath target reflection coefficients. A real data result was presented for a moderately strong high altitude target where the estimate was accurate to within 300 ft. of the true altitude for most of the dwells which validates the simulation results. While the approach presented here accounts for uncertainty in the dwell-to-dwell target reflection coefficients, it does not account for potential mismatch in the intra-dwell target response due to radar calibration errors or to ionospheric effects such as delay spread from polarization dependent propagation paths. This is an area of future investigation.

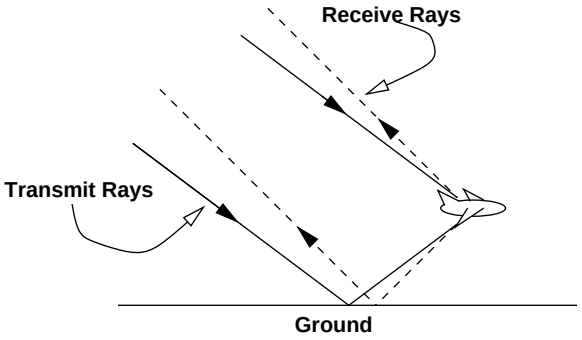

Fig. 1. Micro-multipaths local to aircraft target for transmission and reflection with a bistatic radar.

The authors would like to thank Serafin Rodriguez of NRL in Washington, D.C. for his invaluable assistance with the radar data. The authors also thank Bill Yssel of SPAWAR Systems Center, San Diego, as well as Justin Praschifka and Gordon Frasier of DSTO in Adelaide, Australia for their helpful comments and suggestions.

6. REFERENCES

[1] J. M. Headrick and J. F. Thomason, "Applications of high-frequency radar," *Radio Science*, vol. 33, no. 4, pp. 1045–1054, July-August 1998.

[2] L. F. McNamara, *The Ionosphere: Communications, Surveillance, and Direction Finding*, Krieger Publishing, Melbourne, FL, 1991.

[3] M. A. Papazoglou and J. L. Krolik, "Matched field estimation of aircraft altitude from multiple over-the-horizon radar revisits," *IEEE transactions on Signal Processing*, vol. 47, no. 4, pp. 966–976, April 1999.

[4] M. A. Papazoglou, *Matched Field Altitude Estimation for Over-the-Horizon Radar*, Ph.D. thesis, Duke University, 1998.

[5] A. B. Baggeroer, W.A. Kuperman, and H. Schmidt, "Matched field processing: source localization in correlated noise as an optimum parameter estimation problem," *Journal of the Acoustical Society of America*, vol. 83, pp. 571–587, February 1988.

[6] D. F. Gingras, P. Gerstoft, and N. L. Gerr, "Electromagnetic matched-field processing: Basic concepts and tropospheric simulations," *IEEE Transactions on Antennas and Propagation*, vol. 45, pp. 1536–1545, October 1997.

[7] Raytheon Company, *Relocatable over the horizon radar - system design and operations document*, June 1992, Prepared under contract N00039-90-C-0027.

[8] M. Efe, J. A. Bather, and D. P. Atherton, "An adaptive kalman filter with sequential rescaling of process noise," in *Proceedings of the American Control Conference*, San Diego, CA, June 1999, pp. 3913–3917.

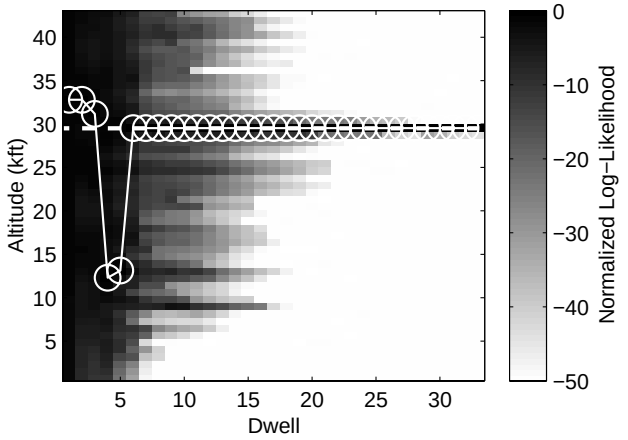

Fig. 2. Log-likelihood vs. dwell for simulated data, true altitude is 29,500 ft., estimated altitude is 29,500 ft.

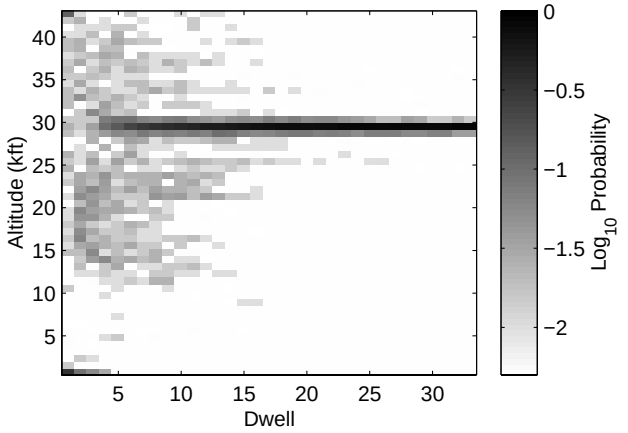

Fig. 3. Log-probability of simulation altitude estimates for 200 realizations at 20 dB SNR for a true altitude of 29,500 ft.

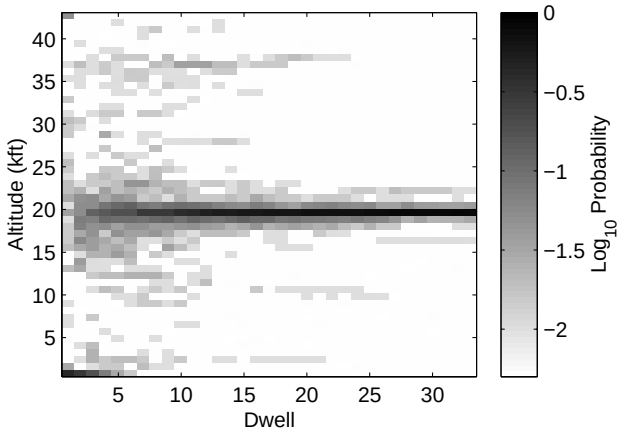

Fig. 4. Log-probability of simulation altitude estimates for 200 realizations at 20 dB SNR for a true altitude of 19,700 ft.

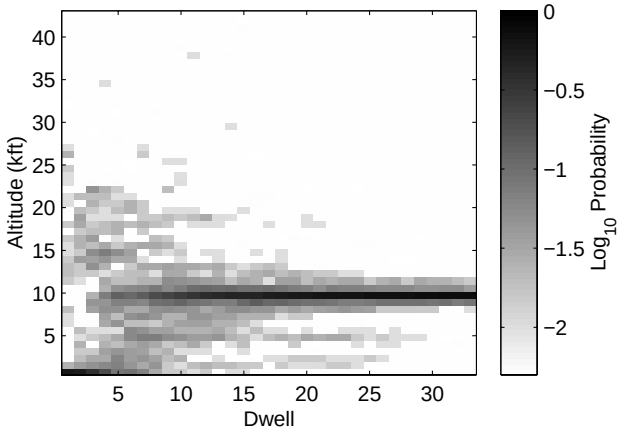

Fig. 5. Log-probability of simulation altitude estimates for 200 realizations at 20 dB SNR for a true altitude of 9,800 ft.

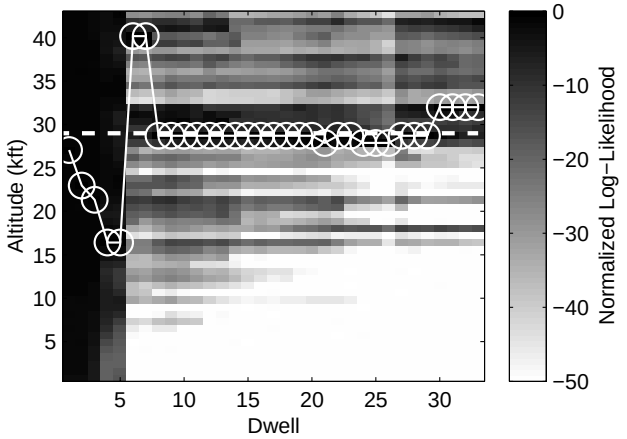

Fig. 6. Real-data log-likelihood vs. dwell, true altitude is 29,000 ft., estimated altitude is 31,900 ft.